HAL
open science

Imaging and Measuring Vesicular Acidification with a Plasma Membrane-Targeted Ratiometric pH Probe

Sophie Michelis, Lydia Danglot, Romain Vauchelles, Andrey S Klymchenko, Mayeul Collot

To cite this version:

Sophie Michelis, Lydia Danglot, Romain Vauchelles, Andrey S Klymchenko, Mayeul Collot. Imaging and Measuring Vesicular Acidification with a Plasma Membrane-Targeted Ratiometric pH Probe. Analytical Chemistry, 2022, 94 (15), pp.5996 - 6003. 10.1021/acs.analchem.2c00574 . hal-03842781

HAL Id: hal-03842781

https://hal.science/hal-03842781v1

Submitted on 7 Nov 2022

HAL is a multi-disciplinary open access archive for the deposit and dissemination of scientific research documents, whether they are published or not. The documents may come from teaching and research institutions in France or abroad, or from public or private research centers.

L'archive ouverte pluridisciplinaire **HAL**, est destinée au dépôt et à la diffusion de documents scientifiques de niveau recherche, publiés ou non, émanant des établissements d'enseignement et de recherche français ou étrangers, des laboratoires publics ou privés.

Imaging and Measuring Vesicular Acidification with a Plasma Membrane-Targeted Ratiometric pH Probe

Sophie Michelis,[1] Lydia Danglot,[2] Romain Vauchelles,[1] Andrey S. Klymchenko,[1] Mayeul Collot[1*]

[1] Laboratoire de Bioimagerie et Pathologies, UMR 7021, CNRS/Université de Strasbourg, 74 route du Rhin, 67401 Illkirch-Graffenstaden, France

[2] Université de Paris, Institute of Psychiatry and Neuroscience of Paris, INSERM U1266, Membrane Traffic in Healthy & Diseased Brain, 75014, Paris, France

KEYWORDS: Plasma Membrane Probe, Cell Trafficking, Ratiometric pH Probe, Ratiometric Imaging, Intracellular Vesicles acidification.

ABSTRACT: Tracking the pH variation of intracellular vesicles throughout the endocytosis pathway is of prior importance to better assess the cell trafficking and metabolism of cells. Small molecular fluorescent pH probes are valuable tools in bioimaging but are generally not targeted to intracellular vesicles or are directly targeted to acidic lysosomes thus not allowing the dynamic observation of the vesicular acidification. Herein we designed Mem-pH, a fluorogenic ratiometric pH probe based on chromenoquinoline with appealing photophysical properties, which targets the plasma membrane (PM) of cells and further accumulates in the intracellular vesicles by endocytosis. The exposition of Mem-pH toward the vesicle's lumen allowed monitoring the acidification of the vesicles throughout the endocytic pathway and enabled the measurement of their pH *via* ratiometric imaging.

INTRODUCTION

The plasma membrane (PM), which plays a central role by delimiting the extracellular environment from the cytoplasm is continuously involved in various pathways of internalization (*e.g.* phagocytosis, pinocytosis, endocytosis). PM generates intracellular vesicles that direct the internalization and trafficking of various biomolecules, fluids, and pathogens in the cell.[1,2] Upon trafficking the intravesicular pH varies depending on the signaling and the endosomal maturation.[3,4] Indeed, while the extracellular media and the cytosol display pH values around 7.0-7.4),[3] the vesicles resulting from the endocytic pathway: early endosomes, late endosomes and lysosomes, respectively display decreasing pH values (down to pH<5).[3] Consequently, the study of intracellular vesicle acidification is of prior importance as alterations of this process lead to pathologies.[5,6,7] Therefore, fluorescent pH probes able to report variation of pH in endosomes and lysosomes, can shed light on healthy and pathological processes in cells.[8, 9]

Among the fluorescent pH probes,[10, 11] ratiometric ones that change their photophysical properties (*e.g.* excitation or emission wavelength, fluorescence lifetime) depending on the pH, are of greatest interest as they enable quantitative measurements of pH values using a robust ratiometric readout independent of the probe local concentration or some instrumental settings.[12] Although ratiometric pH systems based on genetically encoded fluorescent protein, have been developed and proved their efficiency,[13, 14, 15] their use is not straightforward, as they require a transfection step thus leading to heterogeneous samples and toxic effects. pH sensors based on nanoparticles,[16, 17, 18, 19] supramolecular assemblies[20] or nanodevices[21] were also successfully used to probe vesicular acidification, however they suffer from low versatility as they are hardly targetable to precise intracellular compartments and organelles. Conversely, molecular ratiometric pH probes are characterized by their small size and their ease of use. Moreover, they can be easily modified by chemical engineering to quickly incorporate new and adapted features, to target them toward specific organelles,[22, 23] and to tune their photophysical properties.[24] Bright and efficient ratiometric pH probes have been developed with an extended palette of colors, and pKa values,[8, 25] but they often lack functionalizable sites. Therefore, their applications are generally limited to (1) cells without specific targeting,[26, 27, 28, 29, 30] (2) mitochondria due to their cationic nature.[31, 32, 33, 34] or (3) lysosomes by means of tertiary amines for accumulation.[35, 36] However, the latter approach does not allow monitoring the vesicular acidification upon endosomal maturation. We thus hypothesized that a ratiometric pH probe targeted to the PM should be able to study the vesicular acidification from early endosomes to lysosomes.

Although cell surface localized functional probes are recently drawing an increasing attention,[37, 38] only few of them are based on ratiometric pH systems. Various example can be found in the literature either based on FRET between a pH probe and a pH-insensitive fluorophrore,[39] or between dyes through a pH sensitive tetraplex DNA structure (i-motif),[40, 41] or via a system using a nanocluster scaffold.[42] These systems proved their ability to efficiently probe the extracellular pH, however, none of them have been used to track the vesicular acidification upon endocytosis.

In this work, and based on our experience in PM targeted probes, [43, 44, 45, 46, 47, 48, 49] we designed and synthesized Mem-pH, a fluorogenic and ratiometric pH probe targeted to the plasma membrane in order to map the distribution and acidification of the intracellular vesicles by means of ratiometric imaging as well as to quantify pH values in single vesicles.

MATERIALS AND METHODS

Synthesis. All starting materials for synthesis were purchased from Alfa Aesar, Sigma Aldrich or TCI Europe and used as received unless stated otherwise. NMR spectra were recorded on a Bruker Avance III 400 MHz spectrometer. Mass spectra were obtained using an Agilent Q-TOF 6520 mass spectrometer. Synthesis and characterization of Mem-pH is described in the supporting information.

Spectroscopic studies. Absorption spectra were recorded on a Cary 4000 Scan ultraviolet–visible spectrophotometer (Shimadzu UV 2700) and emission spectra on a FluoroMax-4 spectrofluorometer (Horiba Jobin Yvon). For fluorescence

spectra, the emission was collected 10 nm after the excitation wavelength. The absorption and emission spectra were measured in 70% Mc-Ilvaine buffer solution with 30% acetonitrile (ACN). A stock solution of Mem-pH was prepared at 1 mM in DMSO. The Mc-Ilvaine buffers with pH values at 3.01, 3.47, 3.82, 4.21, 4.58, 5.05, 5.43, 5.80, 6.18, 6. 64, 6.97, 7.43, 7.78, 7.98 were prepared according to the standard procedures.[50] The extinction coefficients were determined using the Beer-Lambert law. The quantum yields were determined by the following equation 1:

$$\phi = \phi ref \times \frac{I_{fluo}^{sample}\, d\lambda}{I_{fluo}^{ref}\, d\lambda} \times \frac{OD_{ref}}{OD_{sample}} \times \frac{\eta_{sample}^2}{\eta_{ref}^2} \quad (1)$$

with OD optical density and η refraction index of the solvent. 7-(diethylamino)coumarin-3-carboxylic acid (ϕ = 0.93 in dioxane[51]) and Nile Red (ϕ = 0.91 in dioxane[43]) were used as reference for the determination of the basic form and the acidic form of Mem-pH, respectively. The brightness was determined using the following formula: Brightness = $\phi \times \varepsilon$. For the binding kinetics study, liposomes were used at 100 µM of lipids and Mem-pH at 0.5 µM.

Lipid vesicles. Dioleoylphosphatidylcholine (DOPC) was purchased from Sigma-Aldrich. Large unilamellar vesicles (LUVs) were obtained by the extrusion method as previously described.[52] Briefly, a suspension of multilamellar vesicles was extruded by using a Lipex Biomembranes extruder (Vancouver, Canada). The size of the filters was first 0.2 µm (7 passages) and thereafter 0.1 µm (10 passages). This generates monodisperse LUVs with a mean diameter of 0.11 µm as measured with a Malvern Zetasizer Nano ZSP (Malvern, U.K.). LUVs were labelled by adding 2.5 µL of probe stock solution (200 µM in dimethyl sulfoxide) to a 1 mL solutions of vesicles under stirring while recording the fluorescence intensity at 500 nm. A 20 mM phosphate buffer, pH 7.4, was used in these experiments. Molar ratios of probes to lipids was 1 to 200.

Cellular imaging. KB cells (human epithelial carcinoma cells) were incubated in Dulbecco's Modified Eagle Medium (1 g.L^{-1} glucose), supplemented with 10% fetal bovine solution, 1% L-glutamine and 1% antibiotic solution (penicillin-streptomycin) at 37° C in humidified atmosphere containing 5% CO_2. Before imaging cells were incubated with Mem-pH (1 µM) in opti-MEM for 1h. The cells were then washed with opti-MEM before being imaged. Cells were imaged with a Leica TSC SPE laser scanning confocal microscope with a 63X objective. The green channel corresponds to the basic form of Mem-pH (Excitation: 405 nm, fluorescence signal 450-550 nm), the red channel corresponds to the acidic form of Mem-pH (Excitation: 488 nm, fluorescence signal 500-700 nm). Icy and ImageJ (nih.gov) software were used to process the fluorescence images. The ratiometric images were built using RatioloJ, a plugin for imageJ developed by Romain Vauchelles (details an and principle are available in SI and Figure S8).

Colocalization studies. For colocalization with the PM, cells were incubated at 37°C with Mem-pH (1 µM) in opti-MEM for 1 h before being washed and kept in Opti-MEM. MemBright-640[45] (200 nM) was then added and the cells were imaged right away. For lysosomal colocalization, cells were incubated at 37°C with Mem-pH (1 µM) in Opti-MEM for 1 h, then the probe was washed and kept in Opti-MEM for 24 h incubation at 37°C. The cells were then stained with Cresyl Violet[53] (1 µM) before being washed and kept in Opti-MEM prior to imaging.

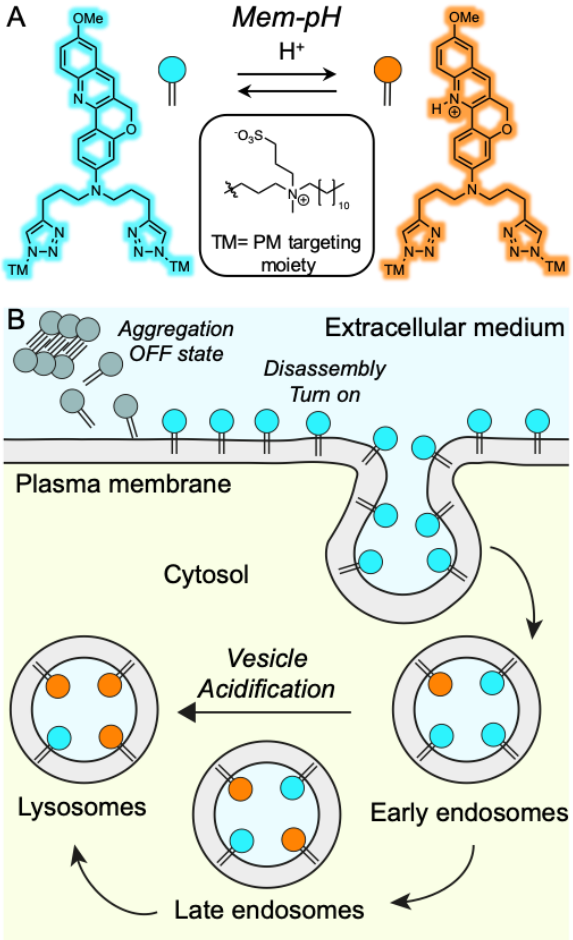

Figure 1. (A) Structure of the PM targeted ratiometric pH probe: Mem-pH. (B) Principle of Mem-pH: The fluorescence is quenched in aqueous media due to aggregation caused quenching, in the presence of cells Mem-pH disassembles, lights up and diffuses in the PM. Upon endocytosis, PM-embedded Mem-pH is internalized within the vesicles and is orientated toward their lumen. Upon vesicle acidification Mem-pH changes its photophysical properties allowing a ratiometric readout of the pH.

Colocalization analysis. For colocalization analysis, cell shape were automatically detected using Hierarchical kmean segmentation with Easy cell shape protocol[54] in Icy software. Colocalization analysis was done using Easy SODA protocol (https://icy.bioimageanalysis.org/protocol/easy-soda-2-colors-1-image/, detailed in Ref[55]) giving the percentage of acidic form associated either with basic form or with lysosomal labeling (Cresyl violet) and *vice-versa* (see table S2). Analysis were done on 4 independent triple labeled pictures, leading to the analysis of more than 2000 positive vesicles.

Calibration of pH values using laser scanning confocal microscope. Mem-pH (10 µM in phosphate-citrate buffer/ACN: 70/30 at different pH values) was placed in 8 wells lab-tek chamber slide. The green and red channels were acquired with the exact same conditions and settings than for cell imaging. The obtained images were processed to obtain an addition binning using imageJ (a square of 100 pixels provided 1 pixel) to enhance the intensity due to the low local concentration of the dye. The obtained binned imaged were sub-

mitted to ratiometric imaging to furnish the color coding of the corresponding pH value.

RESULTS AND DISCUSSION

Design and principle. The design of Mem-pH was first driven by the choice of the ratiometric pH probe. Our criteria of choice were (1) a dedicated excitation wavelength for both the basic and acidic form, (2) decent brightness and (3) pKa in the physiological range (4-8). In 2014, Lin's group reported a pioneer work, where chromenoquinolines derivatives were described as efficient ratiometric fluorescent pH probes.[29] Interestingly, these probes displayed distinctive absorption and emission spectra depending on the pH value. Moreover, one of these probes possessed appealing feature for bioimaging as the basic and acidic form were efficiently excited by the commonly used excitation sources: 405 and 488 nm laser respectively. In 2017, Liu *et al.* extended this study by developing red-shifted chromenoquinolines bearing a morpholine moiety to target lysosomes.[35] Consequently, we intended to design a PM probe based on a chromenoquinoline probe.

In order to enhance the photophysical properties and to install clickable sites, the diethyl amino moiety of the original probe[29] was replaced by a dipentynyl-amino group. We already noticed that this modification led to brighter dyes compared to their diethyl amino analogs,[56] due to the restriction of the N-C σ bond rotation,[57] and the water exclusion phenomenon.[58]

In order to image and monitor the acidification of intracellular vesicles, the ratiometric pH probe was targeted to the PM. In this endeavor we introduced two amphiphilic anchors that proved their efficiency to selectively target the PM (Figure 1A). [44, 45, 46, 47, 49] The PM is continuously involved in the formation of vesicles that progressively get acidified throughout the endocytic pathway.[59] PM probes that insert in the phospholipid bilayer homogeneously stain the PM and, upon incubation, label the vesicles arising from it, as it was shown with polarity-sensitive probe.[60] Due to its amphiphilic nature Mem-pH forms non-emissive soluble aggregates due to aggregation caused quenching (ACQ).[45] Upon contact with the lipophilic membrane, Mem-pH de-aggregates and recovers its fluorescence making it a fluorogenic probe (Figure 1B). Once inserted in the bilayer Mem-pH is exposed to the extracellular environment with a pH around 7.4. After the invagination of the PM, and due to weak tendency to flip-flop,[43, 61] Mem-pH is expected to be expose toward the lumen of the vesicles and is thus ideally positioned to probe their pH variations (Figure 1B). Consequently, Mem-pH can report on the acidification of the vesicle due to a ratiometric readout of its fluorescence signals throughout the endocytic pathway.

Synthesis. Mem-pH was synthesized in 5 steps. First 3-aminophenol was *N*-alkylated by chloropentyne to obtain 1. Then, 1 was involved in a Vilsmeier-Haack formylation giving rise to 2, which was subsequently *O*-propargylated to give 3. The key step of the synthesis is the Povarov reaction involving 3 and *p*-Anisidine and copper iodide as catalyst to yield the clickable key intermediate chromenoquinoline 4. The latter was clicked to the plasma membrane targeting moieties CAZ[44] using the copper(I)-catalyzed alkyne-azide cycloaddition (CuAAC) to finally obtain Mem-pH.

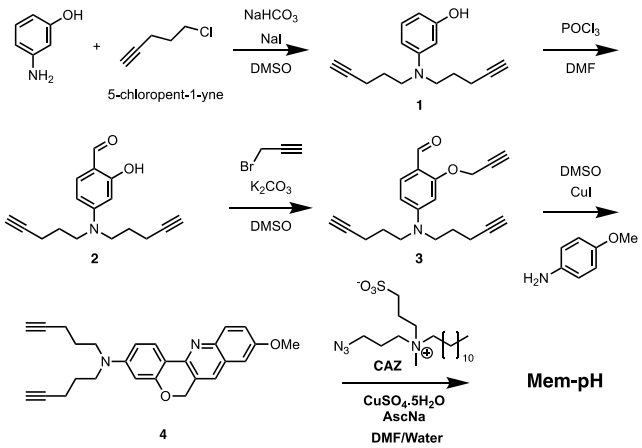

Scheme 1. Synthesis of Mem-pH.

Spectroscopic studies. Mem-pH was obtained in pure form as proven by the HPLC/High resolution mass spectrometry analysis (See SI). Subsequently, the photophysical properties of Mem-pH were studied in various conditions. Both basic and acidic forms of Mem-pH were studied in the presence of triethylamine or trifluoroacetic acid, respectively, and in various solvents with increasing polarity, namely: dioxane, acetonitrile and methanol. As expected Mem-pH exhibited noticeable different photophysical properties in basic and acidic conditions. The basic form is a typical blue emitting dye with maximum absorption wavelength around 395 nm and emission wavelengths in the 460-490 range with a slight positive solvatochromic effect in emission (Figure S1, Table S1).

Table 1. Photophysical properties of Mem-pH

Conditions [a]	λ_{Abs}max (nm)	ε ($M^{-1}.cm^{-1}$)	FMWH [b] (nm)	λ_{Em} max (nm)	FMWH [c] (nm)	ϕ	Brightness ($M^{-1}.cm^{-1}$)
Basic form (pH 8)	397	31,600	56	496	85	0.69	21,800
Acidic form (pH 3)	476	44,200	69	566	93	0.27	12,000

[a] 5 µM in phosphate-citrate buffer/ACN: 70/30

[b] Full Width at Half Maximum depicts the broadness of the absorption peak

[c] Full Width at Half Maximum depicts the broadness of the emission peak

The acidic form absorbs around 477 nm and emits at 560 nm with low effect of the solvent polarity. Interestingly, Mem-pH displayed rather high brightness for both basic and acidic forms, with extinction coefficients up to 30,500 and 46,900 $M^{-1}.cm^{-1}$ and quantum yields up to 0.25 and 0.56, respectively (Table S1). To assess the response of Mem-pH to pH variation, it was studied in phosphate-citrate buffer of different controlled pH values. Acetonitrile was used as a co-solvent for two reasons. First, Mem-pH needs to be solubilized as, due to its amphiphilic nature, it forms nano-aggregates in pure aqueous phases (Figure S2). Then adding acetonitrile helped to mimic the interfacial environment of the probe once embedded in PM lipids. In these conditions Mem-pH absorbed at 397 nm and at 476 nm in basic (pH 8) and acidic conditions (pH 3), respectively, making both forms ≥90% excitable and thus highly compatible with commonly used 405 and 488 nm excitation laser lines (Figure 2A). Surprisingly this aqueous condition enhanced the brightness of the basic form which emits at 496 nm (Figure 2B) and displayed a brightness up to 21,800 $M^{-1}.cm^{-1}$ (Table 1). At low pH values the acidic form of Mem-pH displayed a rather large emission spectrum (Full width at half maximum, FWHM= 93 nm) with an emission maximum at 566 nm (Figure 2C). Although the acidic form displayed a slightly decreased quantum yield in aqueous media (0.27), the latter was compensated by a high extinction coefficient (ε= 44,200 $M^{-1}.cm^{-1}$).

The pKa of Mem-pH was then evaluated using a Hill function fit (Figure 2D) and the Henderson-Hasselbalch equation[29] (figure 2E) to provide values of 4.22 and 4.28, respectively.

The membrane binding kinetic of the probe was assessed by adding Mem-pH to a solution of DOPC vesicles in phosphate buffer (pH 7.4). The results showed a rather fast binding as more than 90% of maximum fluorescence was reached after 10 min (Figure 2F) with a 10-fold fluorescence enhancement upon binding (Figure S3).

Overall Mem-pH possesses attractive features to image pH variations in intracellular vesicles. First, Mem-pH is a fluorogenic probe that binds quickly to model membranes. Its photophysical features allow to image both basic and acidic forms with virtually no crosstalk between acquisition channels and make Mem-pH an ideal candidate to assess pH by ratiometric imaging. Although the pKa (≈4.3) appears low with respect to the minimum pH in vesicles (≈4) the strong signal of the acidic form at pH 4 should allow accurate measurements of pH values in the physical range (pH 4-8).

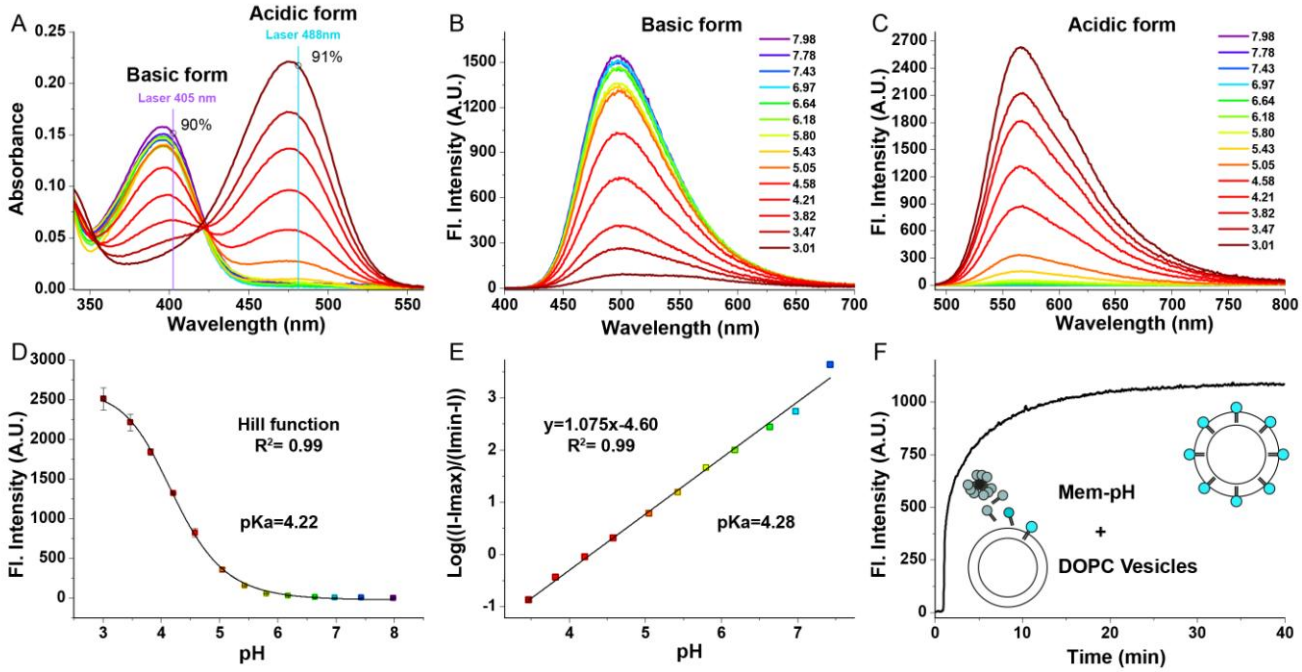

Figure 2. Spectroscopic studies of Mem-pH (5 µM in phosphate-citrate buffer/ACN: 70/30). (A) Absorption spectra of Mem-pH at different pH values. Emission spectra of the basic (B) and acidic (C) forms of Mem-pH at different pH values. Mem-pH was excited at 380 nm (basic form) and 480 nm (acidic form). (D) Fluorescence intensity of the acidic form against different pH values, fitting with the Hill equation provided the pKa value. (E) Determination of pKa using the Henderson-Hasselbalch equation. (F) Evolution of the fluorescence intensity of Mem-pH over the time after addition in the presence of DOPC vesicles (Mem-pH: 500 nM, DOPC: 100 µM in phosphate buffer pH 7.4), λ_{Ex}= 380 nm, the fluorescent signal was collected at 500 nm.

Cellular studies. Prior to the cellular studies, the cytotoxicity of Mem-pH was assessed by MTT assay. The results showed a concentration dependent cytotoxicity with no significant toxicity up to 1 µM (Figure S4). Mem-pH was thus incubated at 1 µM in the presence of KB cells, a cancer cell lines derived from HeLa. In our first investigations using no-wash conditions, Mem-pH was shown to rapidly provide a bright and selective staining of the PM when excited at 405 nm, as proven by colocalization studies using Membright-640 as a PM co-staining (Figure S5). After 1 h incubation the cells were washed and further incubated for 30 min before being imaged by acquisition of both the green and red channels corresponding to the "basic form" and "acidic form" of Mem-pH, respectively (Figure 3A). The signal at the PM remained intense and was not affected by the replacement of the media, indicating strong binding of the dye to PM. Careful observation of the green channel showed appearance of green intracellular dots corresponding to a small number of endocytic vesi-

cles arising from the labeled PM. At this stage, no red signal could be detected (Figure 3B-C). Interestingly, after 3h post-labeling the signal at the PM remained intense (Figure 3D), which could be an asset for cell segmentation, whereas an increasing number of green vesicles was observed compared to 30 min post-labeling. In the red channel, red dots appeared (Figure 3E), probably denoting acidification of some vesicles (Figure 3F). These observations suggest that Mem-pH, when embedded in the vesicular membrane, is orientated toward the lumen of vesicles and could thus get protonated upon vesicular acidification. After 24h post labeling, the PM labeling was less pronounced while the vesicular signal increased due to the continuous involvement of the PM to form new vesicles (Figure 3G).

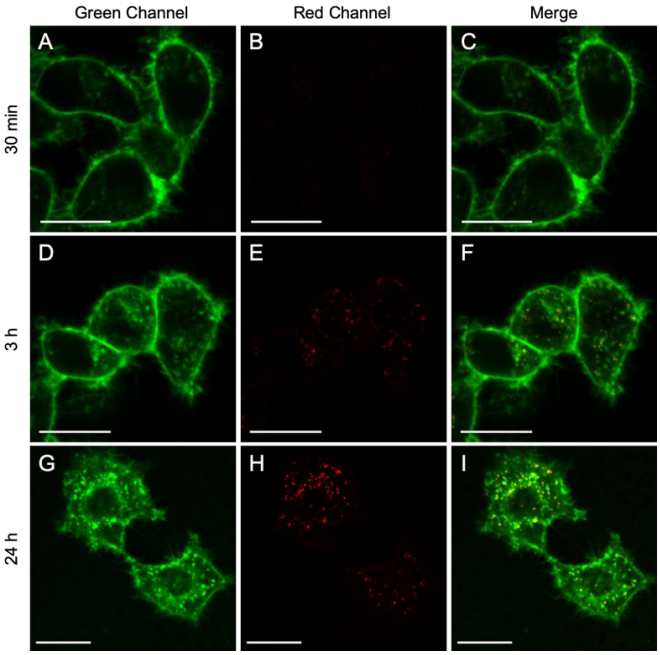

Figure 3. Laser scanning confocal microscopy images of KB cells incubated with Mem-pH (1 µM) for 1 h, washed, and imaged after 30 min (A-C), 3 h (D, F) and 24 h (G-I). The green channel (A, D, G) corresponds to the basic form of Mem-pH (Excitation: 405 nm, fluorescence signal 450-550 nm), the red channel (B, E, H) corresponds to the acidic form of Mem-pH (Excitation: 488 nm, fluorescence signal 500-700 nm). C, F and I are the merge of the green and red channels. Scale bar is 20 µm.

The number and intensity of the red vesicles significantly increased compared to 3h post labeling (Figure 3H) and the merged channel depicted a variety of vesicles displaying various shade of green-yellow-red colors (Figure 3I). These observations are in line with the progressive acidification of intracellular vesicles arising from the maturation of endosome toward lysosomes.[3,4] To verify this hypothesis, 24h post labeling cells were co-stained with a lysosomal marker (Figure S6). To this end, Cresyl violet was chosen to avoid crosstalk as it was not overlapping with Mem-pH (excitation at 560 nm) and it was shown to be a more efficient and reliable lysosomal marker than lysotrackers.[53] Colocalization studies were then performed using Statistical Object Distance Analysis (SODA),[55] and the results can be found in Table S2. First, the vesicles containing the basic form of Mem-pH colocalized with the acid form at 67.6 ± 10.1 % suggesting that after 24h incubation, most vesicles already reached a pH≤5 (pH at which the acidic form start emitting, see figure 2C). Additionally, most of the vesicles contained a fraction of basic form, which is in line with the low pKa of Mem-pH (≈4.3). This low pKa value also explains that 67.1 ± 3.6 % of vesicles containing the basic form colocalized with Cresyl violet. As expected, the vesicles containing the acid form of Mem-pH highly colocalized with Cresyl violet (85.6 ± 3.6 %), proving that the red spot corresponded to the acidification of Mem-pH. The colocalization of Cresyl violet positive spots with the red spots provided a value of 66.8 ± 5.4 % which is explained by the fact that Cresyl violet penetrate the cell to stain all the lysosomes, whereas the acidic form of Mem-pH stain only the lysosomes arising from the initial PM staining. Overall these studies showed that Mem-pH was able to probe endosomal acidification from early endosome to lysosomes.

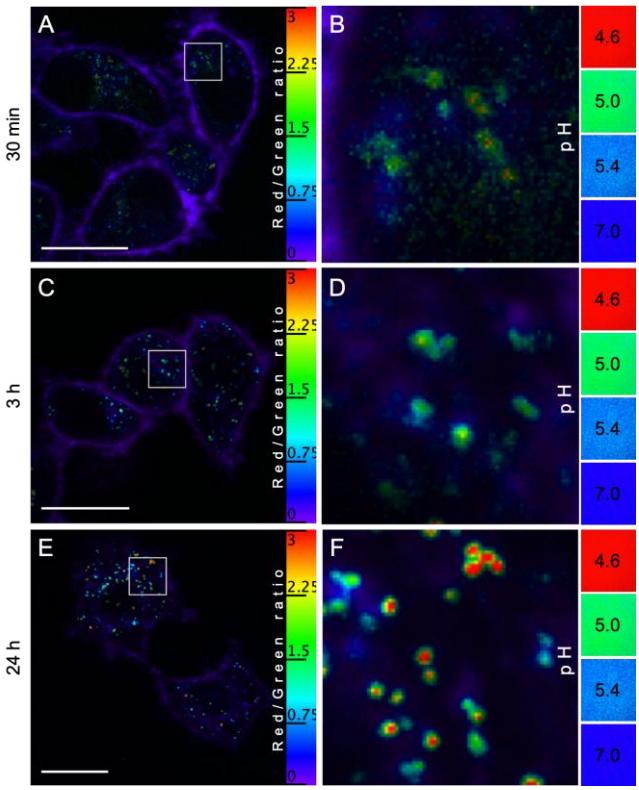

Figure 4. Ratiometric images of KB cells incubated with Mem-pH (1 µM) for 1 h, washed, and imaged after 30 min (A-B), 3 h (C, D) and 24 h (E-F). B, D and F are the zoomed regions corresponding to the white frame in A, C and E, respectively. The value and color-coded ratio were converted to pH value after calibration by imaging Mem-pH (10 µM) in pH buffered solutions.

Ratiometric imaging & determination of vesicles pH. In order to quantify the probe response and analyze the intracellular vesicles' heterogeneity, we performed the ratiometric imaging based on the ratio of pixel intensity from the red and the green channels. The images of Figure 3 were processed to obtain a ratiometric readout. To quantify the pH values of the vesicles, a calibration was performed by imaging solutions of Mem-pH at various pH with the laser scanning microscope and using the same parameters as for cellular imaging.

At 30 min post labeling, the obtained images showed a purplish-blue PM corresponding to a low red/green ratio and a pH higher than 7.0 (figure 4A), suggesting that Mem-pH is exposed to the extracellular medium. At this stage, a dim vesicu-

lar intracellular signal corresponding to pH ≈ 5.0 could already be observed and could be assigned to endosomes[62] (Figure 4B). Interestingly, at 3 h post-labeling the PM kept the same red/green ratio, whereas the green intracellular vesicles appeared in a brighter manner suggesting a continuous accumulation of Mem-pH in the latter (Figure 4C), with low occurrence of the red signal (Figure 4D). At 24 h post-labeling the signal at the PM decreased but kept the same ratio value, corresponding to the extracellular pH. The images displayed numerous and intense intracellular vesicles of various red to green pseudo-colors (Figure 4E). Upon zooming, it appeared that the number of red vesicles corresponding to a pH around 4.6 or lower increased compared to 3 h post labeling (Figure 4F).

From our observations, at 30 min and 3h post-labelling, majority of vesicles presented green pseudo-color, while those displaying a low red/green ratio, *i.e.* pH around 7, were found to be rare, suggesting that once formed the endocytic vesicles (early endosomes) get acidified in a quick manner to reach pH values around 5.0. At 24 h post-labeling, the number of reddish vesicles increased, corresponding to pH <5 which would correspond to lysosomal pH. Interestingly, even after 24 h, some vesicles still displayed colors corresponding to pH values around 7 (Figure 4E), suggesting that the labeled vesicles could be recycled (recycling endosomes) or could change their pH upon their cellular trafficking leading to non-acidic terminal storage lysosome.[63]

CONCLUSION

In this work we postulated that a ratiometric pH probe targeted to the PM could report on the vesicular acidification upon the endocytosis process. To this endeavor, we synthesized Mem-pH, a ratiometric pH probe based on chromenoquinoline and bearing two anchors for targeting PM. Mem-pH was shown to be relatively bright in both its basic and acidic forms with a pKa of ≈4.3. Both of the forms were found to be adapted for the commonly used laser lines at 405 and 488 nm without any cross talk due to well separated both excitation and emission spectra.

Mem-pH quickly and selectively binds to the PM with a fluorescence enhancement of 10-fold, making it an efficient fluorogenic probe. Once labeled, the cells displayed a bright PM in the basic form channel that remain after 24h. Upon incubation, endocytosis occurred and the labeled PM were involved in the formation of vesicles. Owning to it pH sensitivity, Mem-pH was able to report on the vesicular acidification and its ratiometric response allowed to evaluate the pH of the vesicles from early endosomes with 5<pH<6 to lysosomes with pH ≤ 4.6. One should note that the observed kinetics of endosomal acidification on the time scale of hours is slower than that shown in some previous reports (<1h).[62] One reason could be specific endocytic pathway taken by the PM probe, which undergoes relatively slow endocytosis, similar to other PM probes based on the zwitterionic anchor.[45, 60] Further work on the systematic design of pH-sensitive membrane-bound probes will be needed to better understand this phenomenon.

In addition, it is important to point out that Mem-pH showed rather weak photostability during multiple acquisition in microscopy. This was confirmed by spectroscopic studies showing that whereas the acidic form of Mem-pH was rather stable, the basic form displayed significant decrease of intensity upon irradiation compared to coumarin (Figure S7). This feature limits the use of Mem-pH in long term tracking of the same region of interest. However, the ratiometric readout of Mem-pH circumvents this drawback as the ratio value is independent from the photobleaching phenomenon.

In conclusion, Mem-pH combined to ratiometric imaging is an efficient tool to monitor the intracellular vesicles acidification and allows the evaluation of their pH. We believe that Mem-pH can be useful to study the cell trafficking of vesicles, their maturation and recycling to unravel their implication in different pathologies. Finally, Mem-pH could be used to study extracellular vesicles and their role in cancer metastasis.[61]

ACKNOWLEDGMENT

This work was funded by the French National Research Agency (ANR) BrightSwitch 19-CE29-0005-01, ANR-19-CE16-0012, and by FLAG-ERA (grant Senseï by ANR-19-HBPR-0003). The authors would like to thank Dr. Elisabete Cruz Da Silva for her help and Dr. Remi Pelletier for providing DOPC vesicles. The authors also thank the analysis platform (PACSI) and Dr. Sylvette Chasserot for her help in the fluorescence imaging at INCI Strasbourg.

ASSOCIATED CONTENT

Supporting Information. Protocols of synthesis, characterization of new compounds including ^{1}H NMR and ^{13}C NMR and high-resolution mass spectra, and supplementary figures can be found in the supplementary information.
The Supporting Information is available free of charge on the ACS Publications website.

AUTHOR INFORMATION

Corresponding Author

* mayeul.collot@unistra.fr

Author Contributions

The manuscript was written through contributions of all authors. / All authors have given approval to the final version of the manuscript.

REFERENCES

(1) Sigismund, S.; Confalonieri, S.; Ciliberto, A.; Polo, S.; Scita, G.; Di Fiore, P. P. Endocytosis and Signaling: Cell Logistics Shape the Eukaryotic Cell Plan. *Physiol. Rev.* **2012**, *92* (1), 273–366. https://doi.org/10.1152/physrev.00005.2011.

(2) González-Gaitán, M.; Stenmark, H. Endocytosis and Signaling: A Relationship under Development. *Cell* **2003**, *115* (5), 513–521. https://doi.org/10.1016/S0092-8674(03)00932-2.

(3) Casey, J. R.; Grinstein, S.; Orlowski, J. Sensors and Regulators of Intracellular PH. *Nat. Rev. Mol. Cell Biol.* **2010**, *11* (1), 50–61. https://doi.org/10.1038/nrm2820.

(4) Endosome Maturation. *EMBO J.* **2011**, *30* (17), 3481–3500. https://doi.org/10.1038/emboj.2011.286.

(5) Colacurcio, D. J.; Nixon, R. A. Disorders of Lysosomal Acidification—The Emerging Role of v-ATPase in Aging and Neurodegenerative Disease. *Ageing Res. Rev.* **2016**, *32*, 75–88. https://doi.org/10.1016/j.arr.2016.05.004.

(6) Abeliovich, A.; Gitler, A. D. Defects in Trafficking Bridge Parkinson's Disease Pathology and Genetics. *Nature* **2016**, *539* (7628), 207–216. https://doi.org/10.1038/nature20414.

(7) Forgac, M. Vacuolar ATPases: Rotary Proton Pumps in Physiology and Pathophysiology. *Nat. Rev. Mol. Cell Biol.* **2007**, *8* (11), 917–929. https://doi.org/10.1038/nrm2272.

(8) Yue, Y.; Huo, F.; Lee, S.; Yin, C.; Yoon, J. A Review: The Trend of Progress about PH Probes in Cell Application in Recent

Years. *Analyst* **2016**, *142* (1), 30–41. https://doi.org/10.1039/C6AN01942K.

(9) Hou, J.-T.; Ren, W. X.; Li, K.; Seo, J.; Sharma, A.; Yu, X.-Q.; Kim, J. S. Fluorescent Bioimaging of PH: From Design to Applications. *Chem. Soc. Rev.* **2017**, *46* (8), 2076–2090. https://doi.org/10.1039/C6CS00719H.

(10) Han, J.; Burgess, K. Fluorescent Indicators for Intracellular PH. *Chem. Rev.* **2010**, *110* (5), 2709–2728. https://doi.org/10.1021/cr900249z.

(11) Steinegger, A.; Wolfbeis, O. S.; Borisov, S. M. Optical Sensing and Imaging of PH Values: Spectroscopies, Materials, and Applications. *Chem. Rev.* **2020**, *120* (22), 12357–12489. https://doi.org/10.1021/acs.chemrev.0c00451.

(12) Grillo-Hill, B. K.; Webb, B. A.; Barber, D. L. Ratiometric Imaging of PH Probes. In *Methods in Cell Biology*; Elsevier, 2014; Vol. 123, pp 429–448. https://doi.org/10.1016/B978-0-12-420138-5.00023-9.

(13) Richardson, D. S.; Gregor, C.; Winter, F. R.; Urban, N. T.; Sahl, S. J.; Willig, K. I.; Hell, S. W. SRpHi Ratiometric PH Biosensors for Super-Resolution Microscopy. *Nat. Commun.* **2017**, *8* (1), 577. https://doi.org/10.1038/s41467-017-00606-4.

(14) Chin, M. Y.; Patwardhan, A. R.; Ang, K.-H.; Wang, A. L.; Alquezar, C.; Welch, M.; Nguyen, P. T.; Grabe, M.; Molofsky, A. V.; Arkin, M. R.; Kao, A. W. Genetically Encoded, PH-Sensitive MTFP1 Biosensor for Probing Lysosomal PH. *ACS Sens.* **2021**, *6* (6), 2168–2180. https://doi.org/10.1021/acssensors.0c02318.

(15) Perkins, L. A.; Yan, Q.; Schmidt, B. F.; Kolodieznyi, D.; Saurabh, S.; Larsen, M. B.; Watkins, S. C.; Kremer, L.; Bruchez, M. P. Genetically Targeted Ratiometric and Activated PH Indicator Complexes (TRApHIC) for Receptor Trafficking. *Biochemistry* **2018**, *57* (5), 861–871. https://doi.org/10.1021/acs.biochem.7b01135.

(16) Chen, B.; Yang, Y.; Wang, Y.; Yan, Y.; Wang, Z.; Yin, Q.; Zhang, Q.; Wang, Y. Precise Monitoring of Singlet Oxygen in Specific Endocytic Organelles by Super-PH-Resolved Nanosensors. *ACS Appl. Mater. Interfaces* **2021**, *13* (16), 18533–18544. https://doi.org/10.1021/acsami.1c01730.

(17) Despras, G.; Zamaleeva, A. I.; Dardevet, L.; Tisseyre, C.; Magalhaes, J. G.; Garner, C.; Waard, M. D.; Amigorena, S.; Feltz, A.; Mallet, J.-M.; Collot, M. H-Rubies, a New Family of Red Emitting Fluorescent PH Sensors for Living Cells. *Chem. Sci.* **2015**, *6* (10), 5928–5937. https://doi.org/10.1039/C5SC01113B.

(18) Näreoja, T.; Deguchi, T.; Christ, S.; Peltomaa, R.; Prabhakar, N.; Fazeli, E.; Perälä, N.; Rosenholm, J. M.; Arppe, R.; Soukka, T.; Schäferling, M. Ratiometric Sensing and Imaging of Intracellular PH Using Polyethylenimine-Coated Photon Upconversion Nanoprobes. *Anal. Chem.* **2017**, *89* (3), 1501–1508. https://doi.org/10.1021/acs.analchem.6b03223.

(19) Huang, J.; Ying, L.; Yang, X.; Yang, Y.; Quan, K.; Wang, H.; Xie, N.; Ou, M.; Zhou, Q.; Wang, K. Ratiometric Fluorescent Sensing of PH Values in Living Cells by Dual-Fluorophore-Labeled i-Motif Nanoprobes. *Anal. Chem.* **2015**, *87* (17), 8724–8731. https://doi.org/10.1021/acs.analchem.5b01527.

(20) Méndez-Ardoy, A.; Reina, J. J.; Montenegro, J. Synthesis and Supramolecular Functional Assemblies of Ratiometric PH Probes. *Chem. – Eur. J.* **2020**, *26* (34), 7516–7536. https://doi.org/10.1002/chem.201904834.

(21) Modi, S.; Nizak, C.; Surana, S.; Halder, S.; Krishnan, Y. Two DNA Nanomachines Map PH Changes along Intersecting Endocytic Pathways inside the Same Cell. *Nat. Nanotechnol.* **2013**, *8* (6), 459–467. https://doi.org/10.1038/nnano.2013.92.

(22) Xu, W.; Zeng, Z.; Jiang, J.-H.; Chang, Y.-T.; Yuan, L. Discerning the Chemistry in Individual Organelles with Small-Molecule Fluorescent Probes. *Angew. Chem. Int. Ed.* **2016**, *55* (44), 13658–13699. https://doi.org/10.1002/anie.201510721.

(23) Chen, G.; Fu, Q.; Yu, F.; Ren, R.; Liu, Y.; Cao, Z.; Li, G.; Zhao, X.; Chen, L.; Wang, H.; You, J. Wide-Acidity-Range PH Fluorescence Probes for Evaluation of Acidification in Mitochondria and Digestive Tract Mucosa. *Anal. Chem.* **2017**, *89* (16), 8509–8516. https://doi.org/10.1021/acs.analchem.7b02164.

(24) Grimm, J. B.; Tkachuk, A. N.; Xie, L.; Choi, H.; Mohar, B.; Falco, N.; Schaefer, K.; Patel, R.; Zheng, Q.; Liu, Z.; Lippincott-Schwartz, J.; Brown, T. A.; Lavis, L. D. A General Method to Optimize and Functionalize Red-Shifted Rhodamine Dyes. *Nat. Methods* **2020**, *17* (8), 815–821. https://doi.org/10.1038/s41592-020-0909-6.

(25) Di Costanzo, L.; Panunzi, B. Visual PH Sensors: From a Chemical Perspective to New Bioengineered Materials. *Molecules* **2021**, *26* (10), 2952. https://doi.org/10.3390/molecules26102952.

(26) Wang, S.; Fan, Y.; Li, D.; Sun, C.; Lei, Z.; Lu, L.; Wang, T.; Zhang, F. Anti-Quenching NIR-II Molecular Fluorophores for in Vivo High-Contrast Imaging and PH Sensing. *Nat. Commun.* **2019**, *10* (1), 1058. https://doi.org/10.1038/s41467-019-09043-x.

(27) Zhu, S.; Lin, W.; Yuan, L. Development of a Ratiometric Fluorescent PH Probe for Cell Imaging Based on a Coumarin–Quinoline Platform. *Dyes Pigments* **2013**, *99* (2), 465–471. https://doi.org/10.1016/j.dyepig.2013.05.010.

(28) Jun, J. V.; Petersson, E. J.; Chenoweth, D. M. Rational Design and Facile Synthesis of a Highly Tunable Quinoline-Based Fluorescent Small-Molecule Scaffold for Live Cell Imaging. *J. Am. Chem. Soc.* **2018**, *140* (30), 9486–9493. https://doi.org/10.1021/jacs.8b03738.

(29) Huang, W.; Lin, W.; Guan, X. Development of Ratiometric Fluorescent PH Sensors Based on Chromenoquinoline Derivatives with Tunable PKa Values for Bioimaging. *Tetrahedron Lett.* **2014**, *55* (1), 116–119. https://doi.org/10.1016/j.tetlet.2013.10.130.

(30) Li, Y.; Wang, Y.; Yang, S.; Zhao, Y.; Yuan, L.; Zheng, J.; Yang, R. Hemicyanine-Based High Resolution Ratiometric near-Infrared Fluorescent Probe for Monitoring PH Changes in Vivo. *Anal. Chem.* **2015**, *87* (4), 2495–2503. https://doi.org/10.1021/ac5045498.

(31) Wu, M.-Y.; Li, K.; Liu, Y.-H.; Yu, K.-K.; Xie, Y.-M.; Zhou, X.-D.; Yu, X.-Q. Mitochondria-Targeted Ratiometric Fluorescent Probe for Real Time Monitoring of PH in Living Cells. *Biomaterials* **2015**, *53*, 669–678. https://doi.org/10.1016/j.biomaterials.2015.02.113.

(32) Chen, H.; Lin, W.; Jiang, W.; Dong, B.; Cui, H.; Tang, Y. Locked-Flavylium Fluorescent Dyes with Tunable Emission Wavelengths Based on Intramolecular Charge Transfer for Multi-Color Ratiometric Fluorescence Imaging. *Chem. Commun.* **2015**, *51* (32), 6968–6971. https://doi.org/10.1039/C5CC01242B.

(33) Jiang, A.; Chen, G.; Xu, J.; Liu, Y.; Zhao, G.; Liu, Z.; Chen, T.; Li, Y.; James, T. D. Ratiometric Two-Photon Fluorescent Probe for in Situ Imaging of Carboxylesterase (CE)-Mediated Mitochondrial Acidification during Medication. *Chem. Commun.* **2019**, *55* (76), 11358–11361. https://doi.org/10.1039/C9CC05759E.

(34) Li, X.; Hu, Y.; Li, X.; Ma, H. Mitochondria-Immobilized Near-Infrared Ratiometric Fluorescent PH Probe To Evaluate Cellular Mitophagy. *Anal. Chem.* **2019**, *91* (17), 11409–11416. https://doi.org/10.1021/acs.analchem.9b02782.

(35) Liu, X.; Su, Y.; Tian, H.; Yang, L.; Zhang, H.; Song, X.; Foley, J. W. Ratiometric Fluorescent Probe for Lysosomal PH Measurement and Imaging in Living Cells Using Single-Wavelength Excitation. *Anal. Chem.* **2017**, *89* (13), 7038–7045. https://doi.org/10.1021/acs.analchem.7b00754.

(36) Wen, Y.; Zhang, W.; Liu, T.; Huo, F.; Yin, C. Pinpoint Diagnostic Kit for Heat Stroke by Monitoring Lysosomal PH. *Anal. Chem.* **2017**, *89* (21), 11869–11874. https://doi.org/10.1021/acs.analchem.7b03612.

(37) Liu, C.; Gao, X.; Yuan, J.; Zhang, R. Advances in the Development of Fluorescence Probes for Cell Plasma Membrane Imaging. *TrAC Trends Anal. Chem.* **2020**, *133*, 116092. https://doi.org/10.1016/j.trac.2020.116092.

(38) Jia, H.-R.; Zhu, Y.-X.; Duan, Q.-Y.; Wu, F.-G. Cell Surface-Localized Imaging and Sensing. *Chem. Soc. Rev.* **2021**, *50* (10), 6240–6277. https://doi.org/10.1039/D1CS00067E.

(39) Ke, G.; Zhu, Z.; Wang, W.; Zou, Y.; Guan, Z.; Jia, S.; Zhang, H.; Wu, X.; Yang, C. J. A Cell-Surface-Anchored Ratiometric Fluorescent Probe for Extracellular PH Sensing. *ACS Appl. Mater. Interfaces* **2014**, *6* (17), 15329–15334. https://doi.org/10.1021/am503818n.

(40) Ying, L.; Xie, N.; Yang, Y.; Yang, X.; Zhou, Q.; Yin, B.; Huang, J.; Wang, K. A Cell-Surface-Anchored Ratiometric i-Motif Sensor for Extracellular PH Detection. *Chem. Commun.* **2016**, *52* (50), 7818–7821. https://doi.org/10.1039/C6CC03163C.

(41) Zeng, S.; Liu, D.; Li, C.; Yu, F.; Fan, L.; Lei, C.; Huang, Y.; Nie, Z.; Yao, S. Cell-Surface-Anchored Ratiometric DNA Tweezer for Real-Time Monitoring of Extracellular and Apoplastic PH. *Anal. Chem.* **2018**, *90* (22), 13459–13466. https://doi.org/10.1021/acs.analchem.8b03299.

(42) Yang, Y.; Xia, M.; Zhao, H.; Zhang, S.; Zhang, X. A Cell-Surface-Specific Ratiometric Fluorescent Probe for Extracellular PH Sensing with Solid-State Fluorophore. *ACS Sens.* **2018**, *3* (11), 2278–2285. https://doi.org/10.1021/acssensors.8b00514.

(43) Kucherak, O. A.; Oncul, S.; Darwich, Z.; Yushchenko, D. A.; Arntz, Y.; Didier, P.; Mély, Y.; Klymchenko, A. S. Switchable Nile Red-Based Probe for Cholesterol and Lipid Order at the Outer Leaflet of Biomembranes. *J. Am. Chem. Soc.* **2010**, *132* (13), 4907–4916. https://doi.org/10.1021/ja100351w.

(44) Collot, M.; Kreder, R.; Tatarets, A. L.; Patsenker, L. D.; Mely, Y.; Klymchenko, A. S. Bright Fluorogenic Squaraines with Tuned Cell Entry for Selective Imaging of Plasma Membrane vs. Endoplasmic Reticulum. *Chem. Commun.* **2015**, *51* (96), 17136–17139. https://doi.org/10.1039/C5CC06094J.

(45) Collot, M.; Ashokkumar, P.; Anton, H.; Boutant, E.; Faklaris, O.; Galli, T.; Mély, Y.; Danglot, L.; Klymchenko, A. S. MemBright: A Family of Fluorescent Membrane Probes for Advanced Cellular Imaging and Neuroscience. *Cell Chem. Biol.* **2019**, *26* (4), 600-614.e7. https://doi.org/10.1016/j.chembiol.2019.01.009.

(46) Collot, M.; Boutant, E.; Lehmann, M.; Klymchenko, A. S. BODIPY with Tuned Amphiphilicity as a Fluorogenic Plasma Membrane Probe. *Bioconjug. Chem.* **2019**, *30* (1), 192–199. https://doi.org/10.1021/acs.bioconjchem.8b00828.

(47) Collot, M.; Boutant, E.; Fam, K. T.; Danglot, L.; Klymchenko, A. S. Molecular Tuning of Styryl Dyes Leads to Versatile and Efficient Plasma Membrane Probes for Cell and Tissue Imaging. *Bioconjug. Chem.* **2020**, *31* (3), 875–883. https://doi.org/10.1021/acs.bioconjchem.0c00023.

(48) Danylchuk, D. I.; Moon, S.; Xu, K.; Klymchenko, A. S. Switchable Solvatochromic Probes for Live-Cell Super-Resolution Imaging of Plasma Membrane Organization. *Angew. Chem. Int. Ed.* **2019**, *58* (42), 14920–14924. https://doi.org/10.1002/anie.201907690.

(49) Mukherjee, T.; Kanvah, S.; Klymchenko, A. S.; Collot, M. Probing Variations of Reduction Activity at the Plasma Membrane Using a Targeted Ratiometric FRET Probe. *ACS Appl. Mater. Interfaces* **2021**, *13* (34), 40315–40324. https://doi.org/10.1021/acsami.1c11069.

(50) McIlvaine Buffer. *Wikipedia*; 2021.

(51) Chatterjee, A.; Seth, D. Photophysical Properties of 7-(Diethylamino)Coumarin-3-Carboxylic Acid in the Nanocage of Cyclodextrins and in Different Solvents and Solvent Mixtures. *Photochem. Photobiol.* **2013**, *89* (2), 280–293. https://doi.org/10.1111/php.12000.

(52) Hope, M. J.; Bally, M. B.; Webb, G.; Cullis, P. R. Production of Large Unilamellar Vesicles by a Rapid Extrusion Procedure: Characterization of Size Distribution, Trapped Volume and Ability to Maintain a Membrane Potential. *Biochim. Biophys. Acta* **1985**, *812* (1), 55–65.

(53) Ostrowski, P. P.; Fairn, G. D.; Grinstein, S.; Johnson, D. E. Cresyl Violet: A Superior Fluorescent Lysosomal Marker. *Traffic* **2016**, *17* (12), 1313–1321. https://doi.org/10.1111/tra.12447.

(54) Lydia, D. Easy Cell Shape with HK-Means Protocol - Graphical Programming for Icy Software. **2020**. https://doi.org/10.5281/zenodo.4317783.

(55) Lagache, T.; Grassart, A.; Dallongeville, S.; Faklaris, O.; Sauvonnet, N.; Dufour, A.; Danglot, L.; Olivo-Marin, J.-C. Mapping Molecular Assemblies with Fluorescence Microscopy and Object-Based Spatial Statistics. *Nat. Commun.* **2018**, *9* (1), 698. https://doi.org/10.1038/s41467-018-03053-x.

(56) Ponsot, F.; Shen, W.; Ashokkumar, P.; Audinat, E.; Klymchenko, A. S.; Collot, M. PEGylated Red-Emitting Calcium Probe with Improved Sensing Properties for Neuroscience. *ACS Sens.* **2017**, *2* (11), 1706–1712. https://doi.org/10.1021/acssensors.7b00665.

(57) Grimm, J. B.; English, B. P.; Chen, J.; Slaughter, J. P.; Zhang, Z.; Revyakin, A.; Patel, R.; Macklin, J. J.; Normanno, D.; Singer, R. H.; Lionnet, T.; Lavis, L. D. A General Method to Improve Fluorophores for Live-Cell and Single-Molecule Microscopy. *Nat. Methods* **2015**, *12* (3), 244. https://doi.org/10.1038/nmeth.3256.

(58) Hoelzel, C. A.; Hu, H.; Wolstenholme, C. H.; Karim, B. A.; Munson, K. T.; Jung, K. H.; Zhang, H.; Liu, Y.; Yennawar, H. P.; Asbury, J. B.; Li, X.; Zhang, X. A General Strategy to Enhance Donor-Acceptor Molecules Using Solvent-Excluding Substituents. *Angew. Chem. Int. Ed.* **2020**, *59* (12), 4785–4792. https://doi.org/10.1002/anie.201915744.

(59) Sahay, G.; Alakhova, D. Y.; Kabanov, A. V. Endocytosis of Nanomedicines. *J. Controlled Release* **2010**, *145* (3), 182–195. https://doi.org/10.1016/j.jconrel.2010.01.036.

(60) Darwich, Z.; Klymchenko, A. S.; Dujardin, D.; Mély, Y. Imaging Lipid Order Changes in Endosome Membranes of Live Cells by Using a Nile Red-Based Membrane Probe. *RSC Adv.* **2014**, *4* (17), 8481–8488. https://doi.org/10.1039/C3RA47181K.

(61) Hyenne, V.; Ghoroghi, S.; Collot, M.; Bons, J.; Follain, G.; Harlepp, S.; Mary, B.; Bauer, J.; Mercier, L.; Busnelli, I.; Lefebvre, O.; Fekonja, N.; Garcia-Leon, M. J.; Machado, P.; Delalande, F.; López, A. A.; Silva, S. G.; Verweij, F. J.; van Niel, G.; Djouad, F.; Peinado, H.; Carapito, C.; Klymchenko, A. S.; Goetz, J. G. Studying the Fate of Tumor Extracellular Vesicles at High Spatiotemporal Resolution Using the Zebrafish Embryo. *Dev. Cell* **2019**, *48* (4), 554-572.e7. https://doi.org/10.1016/j.devcel.2019.01.014.

(62) Yamashiro, D. J.; Maxfield, F. R. Kinetics of Endosome Acidification in Mutant and Wild-Type Chinese Hamster Ovary Cells. *J. Cell Biol.* **1987**, *105* (6), 2713–2721. https://doi.org/10.1083/jcb.105.6.2713.

(63) Bright, N. A.; Davis, L. J.; Luzio, J. P. Endolysosomes Are the Principal Intracellular Sites of Acid Hydrolase Activity. *Curr. Biol.* **2016**, *26* (17), 2233–2245. https://doi.org/10.1016/j.cub.2016.06.046.
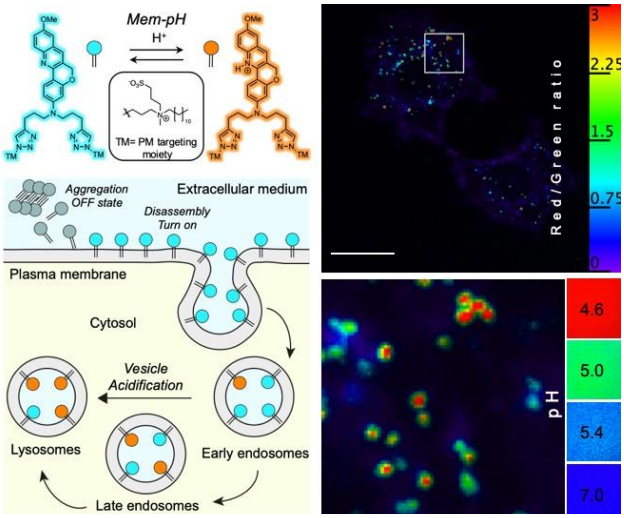
Graphical abstract: